NEUROSCIENCE

REVIEW

M. Straathof et al. / Neuroscience xxx (2021) xxx–xxx

Deuterium Metabolic Imaging of the Healthy and Diseased Brain

Milou Straathof,[a†] Anu E. Meerwaldt,[a†] Henk M. De Feyter,[b] Robin A. de Graaf[b,c] and Rick M. Dijkhuizen[a*]

[a] *Biomedical MR Imaging and Spectroscopy Group, Center for Image Sciences, University Medical Center Utrecht and Utrecht University, Utrecht, the Netherlands*

[b] *Department of Radiology and Biomedical Imaging, Magnetic Resonance Research Center, Yale University School of Medicine, New Haven, CT, USA*

[c] *Department of Biomedical Engineering, Magnetic Resonance Research Center, Yale University, New Haven, CT, USA*

Abstract—Altered brain metabolism contributes to pathophysiology in cerebrovascular and neurodegenerative diseases such as stroke and Alzheimer's disease. Current clinical tools to study brain metabolism rely on positron emission tomography (PET) requiring specific hardware and radiotracers, or magnetic resonance spectroscopy (MRS) involving technical complexity. In this review we highlight deuterium metabolic imaging (DMI) as a novel translational technique for assessment of brain metabolism, with examples from brain tumor and stroke studies. DMI is an MRS-based method that enables detection of deuterated substrates, such as glucose, and their metabolic products, such as lactate, glutamate and glutamine. It provides additional detail of downstream metabolites compared to analogous approaches like fluorodeoxyglucose (FDG)-PET, and can be implemented and executed on clinical and preclinical MR systems. We foresee that DMI, with future improvements in spatial and temporal resolutions, holds promise to become a valuable MR imaging (MRI) method for non-invasive mapping of glucose uptake and its downstream metabolites in healthy and diseased brain.

Key words: MRI, deuterium, MR spectroscopy, brain metabolism, stroke, tumor.

INTRODUCTION

While contributing to only 2% of an average body weight, the brain accounts for at least 20% of the body's energy metabolism in rest (Mink et al., 1981). To ensure normal brain function, which is dependent on highly energy-consuming signaling between neurons (Harris et al., 2012), continuous supply of oxygen and glucose is required. Unlike most other organs, the brain has very limited capability for glucose storage (in the form of glycogen). If blood supply to the brain is interrupted, for example after stroke, metabolic functioning of brain cells rapidly declines, leading to temporary or permanent loss of brain functions. In the last decades, *in vivo* studies on brain energy metabolism have significantly contributed to the understanding of brain physiology and pathology. Many of these studies have made use of specialized imaging techniques to map (changes in) the brain's metabolic status.

Clinical imaging tools for assessment of active brain metabolism generally make use of positron emission tomography (PET) or magnetic resonance (MR) spectroscopy (MRS) methods. ^{18}F-fluorodeoxyglucose (FDG)-PET can be considered the gold standard for metabolic imaging in the clinic. MRS methods, specifically ^{13}C-MRS for measurement of active metabolism, have been successfully applied in (small) animal studies, but remain rarely used in clinical settings due to their technical complexity. Recently, a novel ^{2}H-MR-based method, termed deuterium (^{2}H) metabolic imaging (DMI) (De Feyter et al., 2018), has been introduced, which has the potential of broad application for *in vivo* mapping of active brain metabolism in preclinical and clinical settings.

DMI of active metabolism involves a MR spectroscopic imaging approach for *in vivo* detection of infused or ingested deuterium-labelled glucose and its metabolites in tissue. In contrast to MRS approaches without isotope-labeled precursors, DMI informs on active uptake and formation of metabolites. This reduces ambiguity and possible interference arising

*Corresponding author. Address: Biomedical MR Imaging and Spectroscopy Group, Center for Image Sciences, University Medical Center Utrecht, Heidelberglaan 100, 3584 CX Utrecht, the Netherlands. Fax: +31-30-2535561.

E-mail address: r.m.dijkhuizen@umcutrecht.nl (R. M. Dijkhuizen).

† Shared first author.

Abbreviations: ATP, adenosine triphosphate; CMR_{Glc}, cerebral glucose metabolic rate; DMI, deuterium metabolic imaging; FDG, ^{18}F-fluorodeoxyglucose; GBM, glioblastoma multiforme; Glc, glucose; Glx, glutamate & glutamine; Lac, lactate; MCA, middle cerebral artery; MR, magnetic resonance; MRI, magnetic resonance imaging; MRS, magnetic resonance spectroscopy; PET, positron emission tomography; TCA, tricarboxylic acid; V_{TCA}, tricarboxylic acid cycle flux.

https://doi.org/10.1016/j.neuroscience.2021.01.023
0306-4522/

from metabolic products that are already present in the tissue of interest. ^{1}H-MRS, for example, is able to detect lactate in tissue but cannot differentiate between actively and previously formed lactate. In 2017, Lu et al. (2017) demonstrated how ^{2}H-MRS at high magnetic field strength could be applied to quantify whole-brain cerebral glucose metabolic rate (CMR_{Glc}) and tricarboxylic acid (TCA) cycle flux (V_{TCA}) in rats. The authors were able to differentiate metabolic activity by modulating depth of anesthesia, showing the sensitivity of ^{2}H-MRS in detecting changes in brain energy metabolism. The term DMI was subsequently introduced by De Feyter et al., who acquired localized ^{2}H spectroscopic information from different regions in the brain and liver in rats and humans following infusion or oral intake of deuterated glucose or acetate (De Feyter et al., 2018). They showed that tumor tissue could be identified based on abnormal metabolic activity (e.g. detection of the Warburg effect (Warburg et al., 1924)) in a rat glioma model as well as in patients with a glioblastoma (further outlined below). In addition, they measured ^{2}H-glycogen storage in rodent and human liver. Other recent studies have described applications of DMI outside the brain, with increased temporal resolution in investigating glycolytic flux in a mouse lymphoma model (Kreis et al., 2020), and for detection of glucose uptake and metabolism in brown adipose tissue in rats (Riis-Vestergaard et al., 2020).

In this review, we introduce the methodology of DMI for mapping active brain metabolism, provide examples of application in brain disease studies, and discuss advantages and challenges in comparison with other metabolic neuroimaging techniques.

DMI METHODOLOGY

MRI is typically based on detection of the proton (^{1}H) signal, originating mostly from water, which is highly abundant in biological tissue, and fat. In contrast, DMI is sensitized to detection of deuterium (^{2}H), a stable hydrogen isotope with a very low natural abundance (0.0115%) (Harris et al., 2001), which results in a very weak endogenous ^{2}H-MR signal from biological tissues. ^{2}H-MRI has been previously applied for measurement of blood flow in animal brain based on the washout of intraarterially injected deuterated saline (Detre et al., 1990). The recent DMI studies on brain energy metabolism were combined with administration of deuterated glucose ([6,6]-$^{2}H_2$-glucose) or acetate ($^{2}H_3$-acetate). Deuterated substrates can be injected systemically, which is the standard route of administration for animal studies, but it may also be delivered orally by drinking a solution of the deuterated substrate, as a more convenient approach in studies with human subjects. Concentrations of 0.5–2 g deuterated substrate per kg body weight have been shown to be sufficient for clear *in vivo* detection of downstream metabolites (De Feyter et al., 2018). Controlled intravenous infusion is recommended, however, for accurate quantification of absolute metabolic rates.

DMI data can be relatively easily obtained with a simple radiofrequency pulse-acquire approach, combined with 3D phase-encoding magnetic field gradients for spatial localization (De Feyter et al., 2018). Effort may be required, however, to adapt existing clinical MR scanners for DMI due to system limitations and the need for multi-nuclei amplifiers and radiofrequency coils. Since deuterium resonates at a relatively low MR frequency (e.g., 61.4 MHz vs. 400 MHz for proton, at 9.4 T), DMI is comparatively insensitive to inhomogeneities in the static magnetic field. Furthermore, strategies to suppress unwanted signals from water or fat with radiofrequency pulses, as frequently applied in ^{1}H MR spectroscopic imaging studies, are unnecessary because of the low natural abundance of deuterium in water and fat. *In vivo* T_1 values of deuterated glucose and its downstream metabolites at 4 T and 11.7 T range approximately from 60 to 350 ms, whereas T_2 values vary approximately between 10 and 80 ms (De Feyter et al., 2018). De Graaf et al. (2020) have recently shown that the sensitivity of ^{2}H-MR measurements exceeds that of ^{13}C-MR measurements due to the shorter T_1's and T_2's, and the larger intrinsic magnetic moment. In addition, DMI scales supralinear with the external magnetic field, thus favoring studies at the highest available magnet field strengths. Further details on DMI methodology, including discussion of magnetic field dependence and efficiency of radiofrequency transmission, can be found in papers by De Feyter et al. (2018) and De Graaf et al (2020).

Metabolite concentrations can be determined from the ^{2}H-MRS signals following spectral fitting and execution of a quantification algorithm. Information on dynamic metabolite changes can be used to calculate CMR_{Glc} and V_{TCA} based on a kinetic model, which requires relatively fast DMI acquisition. The feasibility of quantitative measurement of metabolic fluxes was recently demonstrated in a murine tumor model by Kreis et al. (2020), who executed DMI with a temporal resolution of 10 min.

Fig. 1A shows a typical DMI spectrum acquired from a healthy rat brain after ca. 1 h infusion of [6,6]-$^{2}H_2$-glucose. The spectrum reveals three clear peaks that represent the ^{2}H resonance signals from water, glucose and the combined pool of glutamate and glutamine (Glx). The ^{2}H-glucose signal at a chemical shift of 3.8 ppm reflects the administered glucose that was taken up by the brain (unphosphorylated and phosphorylated glucose pool). The ^{2}H-Glx signal at 2.4 ppm arose from processing of pyruvate. Pyruvate is the product of glycolysis in the TCA cycle, reflecting oxidative phosphorylation in the brain. The source of the ^{2}H-water signal at 4.7 ppm includes naturally abundant ^{2}H-water and actively formed ^{2}H-water as an end-product of the TCA cycle in the brain and other organs. A lactate signal at 1.3 ppm was indistinguishable since anaerobic glycolysis is minimal in the healthy brain. Because DMI data were acquired in spectroscopic imaging mode, brain metabolite maps could be reconstructed based on spatial information of individual metabolite levels (see Fig. 1B, D).

BRAIN DMI STUDIES

Cellular energy metabolism can be studied from the uptake, breakdown and downstream processing of

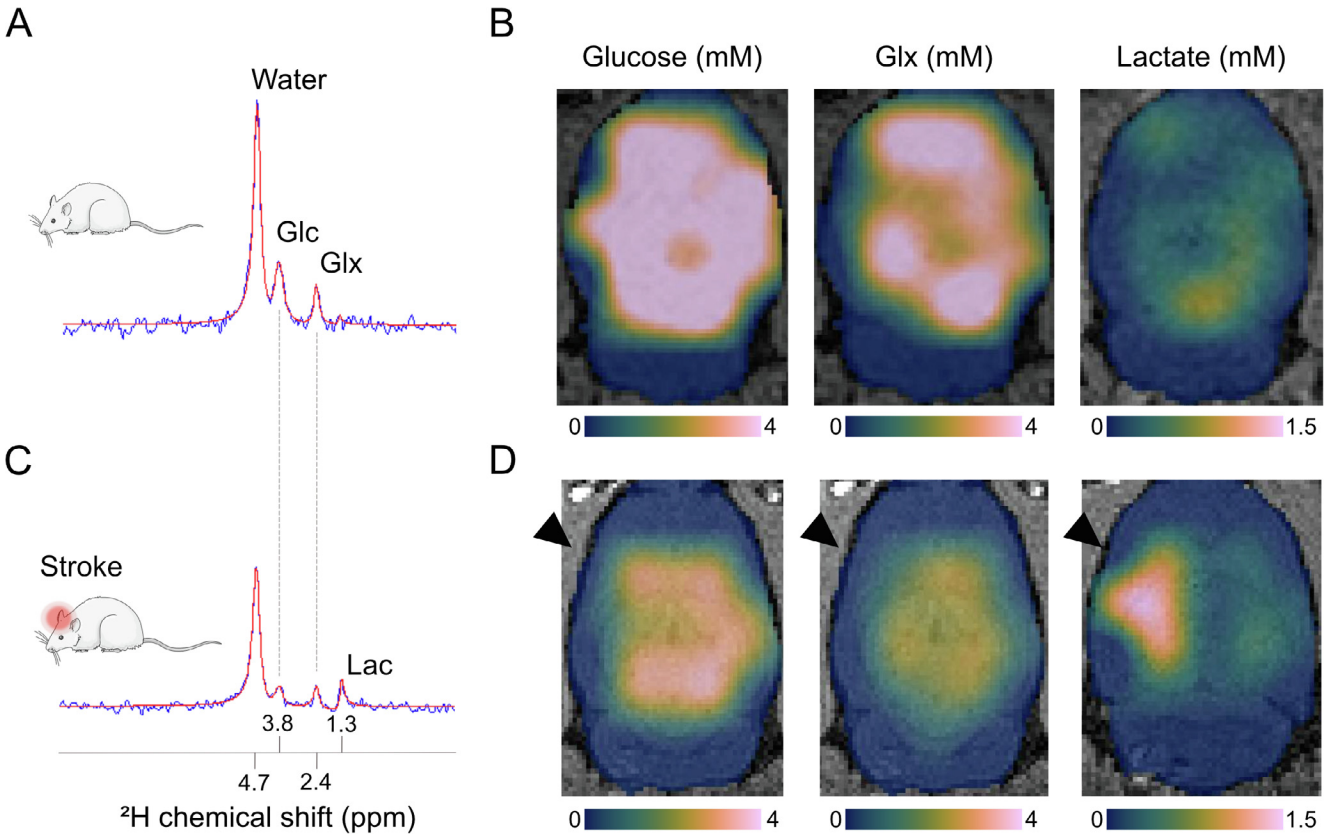

Fig. 1. DMI captures altered glucose metabolism after ischemic stroke in rats. We acquired steady state DMI data at 9.4 T with $3 \times 3 \times 3$ mm^3 = 27 μl nominal spatial resolution in approximately 35 min (repetition time = 400 ms; 8 averages). **(A)** A typical single-voxel DMI spectrum from a healthy rat brain acquired at 60–90 min after start of intravenous infusion with ^{2}H-labeled glucose (1.95 g/kg in 120 min). **(B)** Maps of glucose uptake and metabolic products, i.e. glutamate and glutamine (Glx) and lactate, across the healthy rat brain reveal even distribution of glucose delivery and uptake and oxidative phosphorylation (reflected by the Glx pool), while anaerobic glycolysis (i.e. lactate formation) is minimal. **(C)** A DMI spectrum from a single-voxel placed in a rat's ischemic brain hemisphere shortly after unilateral middle cerebral artery occlusion shows active lactate formation, indicative of anaerobic glucose metabolism. The infusion of ^{2}H-labeled glucose was started directly after occlusion of the middle cerebral artery. **(D)** Acutely after stroke induction, we observed lactate formation in and around the ischemic lesion coupled with reduction in oxidative phosphorylation indicated by a lowered Glx signal. In **(B)** and **(D)**, color-coded (Crameri, 2020) glucose and metabolite maps, expressed in millimolar concentrations, are overlaid on T_2-weighted anatomical MR images of the brain. The black arrowheads mark the ischemic hemisphere. Abbreviations: Glc = glucose, Glx = glutamate & glutamine, Lac = lactate.

glucose. After glycolysis, pyruvate can enter the TCA cycle, where its metabolic breakdown leads to efficient production of adenosine triphosphate (ATP) via oxidative phosphorylation. When there is lack of oxygen, glycolysis is anaerobic and pyruvate is converted into lactate instead of entering the TCA cycle. However, this may also occur under aerobic conditions, which was first described by Otto Warburg, referring to the abnormal metabolic pattern observed in tumor cells (Warburg et al., 1924). This glycolytic shift has been linked to cancer aggressiveness and can assist in characterization of brain tumors (Hollingworth et al., 2006). De Feyter et al. (2018) used DMI to map glycolysis and oxidative phosphorylation across the brain in rats and patients with a glioblastoma (Fig. 2). They measured an increased ratio of lactate over Glx formation in tumor tissue, which is characteristic of the Warburg effect.

Impaired glycolysis, for example as a result of lack of glucose or oxygen supply, occurs in many brain diseases, including stroke, Alzheimer's disease and traumatic brain injury (Siesjö, 1992; Cunnane et al., 2020). We have recently applied DMI to detect anaerobic glycolysis in a rodent ischemic stroke model. Stroke is one of the main causes of death and disability worldwide. Ischemic stroke, caused by the occlusion of a major cerebral artery, accounts for more than 80% of all stroke types. During the first hours of ischemic stroke, the limited availability of oxygen forces cells to switch to anaerobic glycolysis resulting in lactate formation, associated pH decreases, limited ATP production and eventually cell death (Siesjö, 1992). We found that unilateral occlusion of the middle cerebral artery (MCA) in rats led to active ^{2}H-lactate formation from infused ^{2}H-glucose in and around the ischemic stroke lesion immediately following MCA occlusion (Fig. 1C, D). This finding was reflective of residual blood flow, preserved glucose uptake and anaerobic glucose metabolism. In addition, a lower Glx signal in ^{2}H MR spectra from the lesion site indicated a reduction in oxidative phosphorylation. These data demonstrate that DMI can be used for detection of disturbances in brain energy metabolism as a result of cerebral ischemia.

Please cite this article in press as: Straathof M et al. Deuterium Metabolic Imaging of the Healthy and Diseased Brain. Neuroscience (2021), https://doi.org/10.1016/j.neuroscience.2021.01.023

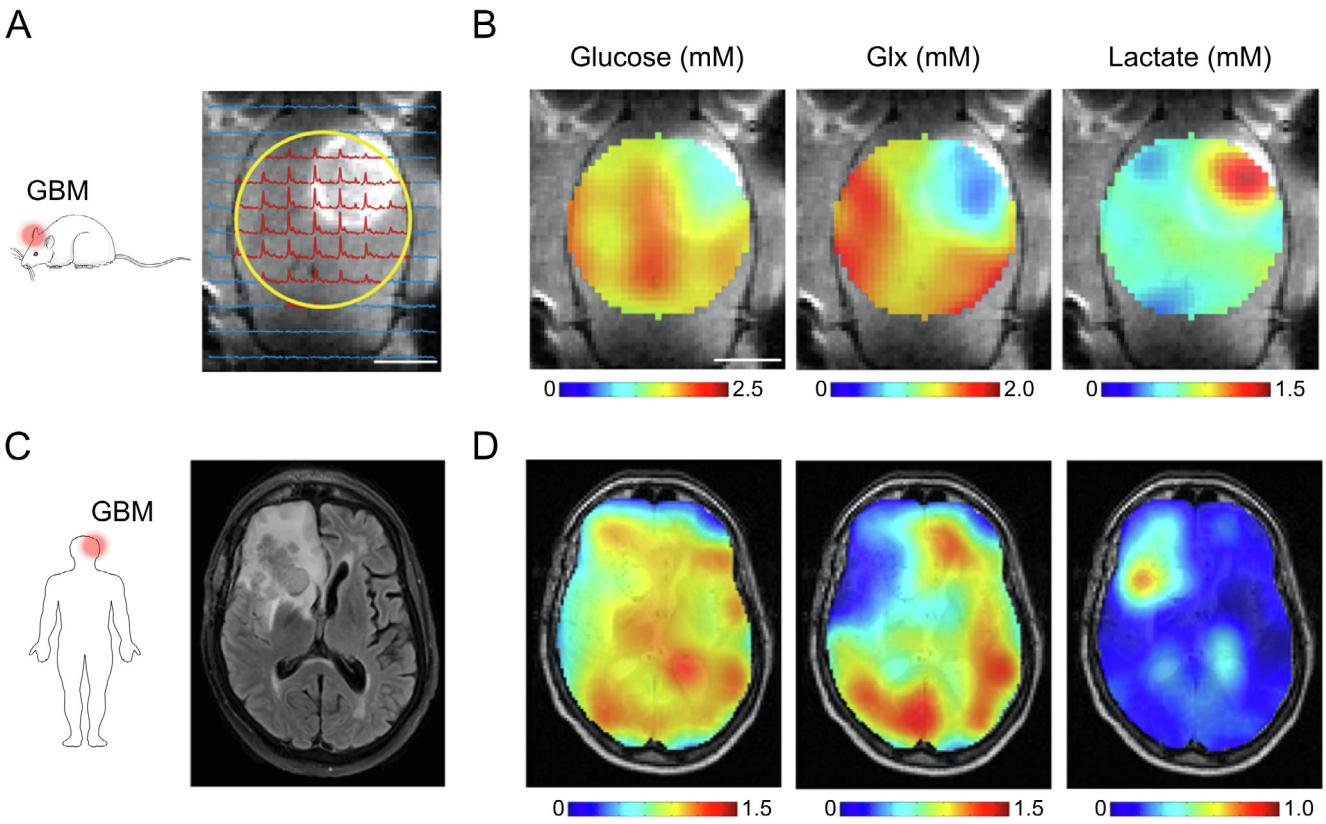

Fig. 2. DMI depicts the Warburg effect in experimental and clinical glioblastoma multiforme (GBM). **(A)** Contrast-enhanced T_1-weighted MRI shows hyperintense signal from tumor tissue in a rat glioma model. Surface radiofrequency coil position for DMI (yellow circle) and localized ^{2}H MR spectra are overlaid onto the MR image. **(B)** Maps of glucose uptake and downstream metabolites, i.e. glutamate and glutamine (Glx) and lactate, reveal active Warburg effect in and around the brain tumor after intravenous infusion of 1.95 g [6,6′]-$^2H_2$-glucose per kg body weight. **(C)** Standard-of-care T_2-weighted fluid-attenuated inversion recovery MR image from a patient diagnosed with GBM in the right frontal lobe. **(D)** Glucose and metabolite maps overlaid onto T_2-weighted MRI show lower levels of ^{2}H-labeled Glx and higher concentration of ^{2}H-labeled lactate in and around the tumor lesion compared to normal-appearing brain tissue, similar to the metabolite maps from the rat glioma model in **(B)**. Subjects orally ingested 0.60–0.75 g [6,6′]-$^2H_2$-glucose per kg body weight, with a maximum of 60 g. Color-coded glucose, Glx and lactate maps are expressed in millimolar concentrations. Abbreviations: Glc = glucose, Glx = glutamate & glutamine, Lac = lactate. Figure adapted from De Feyter et al. (2018) with authors' permission.

COMPARABLE METABOLIC IMAGING TECHNIQUES

Currently, FDG-PET is the metabolic imaging method of choice for detecting altered metabolism in cancer patients. In addition, FDG-PET can be clinically applied for diagnosis of other pathological conditions involving infection, inflammation or neurodegenerative disease. FDG is a glucose analogue, which, similar to glucose, is taken up by living cells through glucose transporter membrane proteins and subsequently phosphorylated by the enzyme hexokinase. Contrary to phosphorylated glucose, phosphorylated FDG does not undergo further downstream processing via glycolysis, and remains 'trapped' within the cell, which makes it a suitable imaging marker for glucose uptake. FDG uptake can be related to tumor grade and proliferation as well as to treatment response, based on enhanced utilization of glucose, upregulation of hexokinase and increased expression of glucose transporters in tumor-associated cells (Smith, 1998). Reduced FDG uptake, due to reduced blood supply or cell loss and reflective of ischemia or tissue degeneration, may be detected in other brain pathologies.

At present DMI scans cannot be obtained with similar spatial resolution as FDG-PET scans, which remains an important hurdle for broad clinical implementation. Nevertheless, DMI offers appealing advantages over FDG-PET. First, DMI does not require radiochemistry and can be considered non-invasive. Second, unlike FDG-PET, DMI can provide information on glycolysis end-products as well as downstream mitochondrial function and oxidative phosphorylation. Third, DMI can be acquired in a single scan session together with anatomical MRI. Fourth, DMI is not dependent on specialized personnel and procedures inherent to using radioactive isotopes, making it more cost-efficient compared to FDG-PET.

Already for decades, MRS approaches have been applied for non-invasive detection of biochemical changes in brain pathologies, including tumors and stroke (Kauppinen and Williams, 1994; Öz et al., 2014). ^{13}C-MRS measurements combined with administration of ^{13}C-labeled substrates, such as glucose, acetate or lac-

tate, offer a powerful non-invasive means for assessment of neurotransmitter function coupled with energy metabolism (Rothman et al., 2011; Sonnay et al., 2017). This has provided original information on glutamate-glutamine neurotransmitter cycling and V_{TCA}. Compared to ^{2}H-metabolites, ^{13}C-metabolites have long T_1 relaxation times, which necessitates longer MRS sampling times to achieve equivalent detection sensitivity. While sensitivity may be improved through indirect ^{1}H/^{13}C-MRS measurements, clinical applications are hampered due to the technical complexity thereof (De Feyter et al., 2018). Furthermore, a key challenge in ^{1}H MR spectroscopic imaging studies is suppression of the endogenous background signal from water and lipids. Particularly extracranial subcutaneous fat affects metabolite detection in outer brain areas, such as the cerebral cortex. Yet, compared to DMI, ^{13}C-MRS offers high spectral resolution and enables more specific detection of metabolites, such as glutamate and glutamine, which lends favorable opportunities for advanced metabolic modeling approaches.

Recent introduction of PET/MR systems have opened up opportunities for simultaneous FDG-PET and MRS imaging, allowing complementary measurements of glucose uptake and downstream metabolism (Gutte et al., 2015). However, PET/MR systems are (still) scarce, and processing of multimodal imaging data is not straightforward. DMI offers an attractive alternative as it allows straightforward execution of studies on downstream glucose metabolism on widely available (clinical) MR systems.

The low natural abundance of deuterium in the body opens the possibility of using DMI in conjunction with ingested or infused deuterated substrates to provide quantitative, non-invasive mapping of active metabolism *in vivo*. This non-invasive technique can be implemented and executed on preclinical and clinical MR systems, and therefore holds great promise for translational studies. We foresee applications for DMI in a broad spectrum of pathologies, in which measurement of brain energy metabolism can contribute to (preclinical) elucidation of pathophysiology or (clinical) diagnosis and outcome prediction. In addition, its usage may be extended to monitoring of responses to treatments aimed at modulating cell metabolism. Moreover, combination of DMI with functional imaging techniques can help to gain insights into the tight interplay between neurovascular function, neurotransmission and neurometabolism in health and disease. To advance the accuracy and speed of assessments with DMI to levels comparable to PET, methodological advancements should be directed towards improvement of spatial and temporal resolution, while preserving sufficient spectral resolution.

ACKNOWLEDGEMENTS

This work was supported by the Netherlands Organization for Scientific Research (VICI 016.130.662 and Graduate Programme 022.006.001); and the National Institutes of Health (NIMH R01-MH095104 and NIBIB R01-EB025840).

REFERENCES

Crameri F (2020) Scientific colour maps. Zenodo. https://doi.org/10.5281/zenodo.4153113.

Cunnane SC, Trushina E, Morland C, Prigione A, Casadesus G, Andrews ZB, Beal MF, Bergersen LH, Brinton RD, de la Monte S, Eckert A, Harvey J, Jeggo R, Jhamandas JH, Kann O, la Cour CM, Martin WF, Mithieux G, Moreira PI, Murphy MP, Nave K-A, Nuriel T, Oliet SHR, Saudou F, Mattson MP, Swerdlow RH, Millan MJ (2020) Brain energy rescue: an emerging therapeutic concept for neurodegenerative disorders of ageing. Nat Rev Drug Discov 19:609–633. https://doi.org/10.1038/s41573-020-0072-x.

De Feyter HM, Behar KL, Corbin ZA, Fulbright RK, Brown PB, McIntyre S, Nixon TW, Rothman DL, De Graaf RA (2018) Deuterium metabolic imaging (DMI) for MRI-based 3D mapping of metabolism in vivo. Sci Adv 4:1–12. https://doi.org/10.1126/sciadv.aat7314.

de Graaf RA, Hendriks AD, Klomp DWJ, Kumaragamage C, Welting D, Arteaga de Castro CS, Brown PB, McIntyre S, Nixon TW, Prompers JJ, De Feyter HM (2020) On the magnetic field dependence of deuterium metabolic imaging. NMR Biomed 33:1–9. https://doi.org/10.1002/nbm.4235.

Detre JA, Subramanian VH, Mitchell MD, Smith DS, Kobayashi A, Zaman A, Leigh JS (1990) Measurement of regional cerebral blood flow in cat brain using intracarotid 2H2O and 2H NMR imaging. Magn Reson Med 14:389–395. https://doi.org/10.1002/mrm.1910140223.

Gutte H, Hansen AE, Larsen MME, Rahbek S, Henriksen ST, Johannesen HH, Ardenkjaer-Larsen J, Kristensen AT, Hojgaard L, Kjaer A (2015) Simultaneous hyperpolarized 13C-pyruvate MRI and 18F-FDG PET (HyperPET) in 10 dogs with cancer. J Nucl Med 56:1786–1792. https://doi.org/10.2967/jnumed.115.156364.

Harris J, Jolivet R, Attwell D (2012) Synaptic energy use and supply. Neuron 75:762–777. https://doi.org/10.1016/j.neuron.2012.08.019.

Harris, R.K., Becker, E.D., Cabral de Menezes, S.M., Goodfellow, R., Granger, P., 2001. NMR nomenclature: nuclear spin properties and conventions for chemical shifts. IUPAC Recommendations 2001. Solid State Nucl Magn Reson 22,458–483. https://doi: 10.1006/snmr.2002.0063.

Hollingworth W, Medina L, Lenkinski R, Shibata D, Bernal B, Zurakowski D, Comstock B, Jarvik J (2006) A systematic literature review of magnetic resonance spectroscopy for the characterization of brain tumors. Am J Neuroradiol 27:1404–1411.

Kauppinen RA, Williams SR (1994) Nuclear magnetic resonance spectroscopy studies of the brain. Prog Neurobiol 44:87–118. https://doi.org/10.1016/0301-0082(94)90058-2.

Kreis F, Wright AJ, Hesse F, Fala M, Hu DE, Brindle KM (2020) Measuring tumor glycolytic flux in vivo by using fast deuterium MRI. Radiology 294:289–296. https://doi.org/10.1148/radiol.2019191242.

Lu M, Zhu X-H, Zhang Yi, Mateescu G, Chen W (2017) Quantitative assessment of brain glucose metabolic rates using in vivo deuterium magnetic resonance spectroscopy. J Cereb Blood Flow Metab Off J Int Soc Cereb Blood Flow Metab 37:3518–3530. https://doi.org/10.1177/0271678X17706444.

Mink JW, Blumenschine RJ, Adams DB (1981) Ratio of central nervous system to body metabolism in vertebrates: its constancy and functional basis. Am J Physiol-Regul Integr Comp Physiol 241:R203–R212. https://doi.org/10.1152/ajpregu.1981.241.3.R203.

Öz G, Alger JR, Barker PB, Bartha R, Bizzi A, Boesch C, Bolan PJ, Brindle KM, Cudalbu C, Dinçer A, Dydak U, Emir UE, Frahm J, González RG, Gruber S, Gruetter R, Gupta RK, Heerschap A, Henning A, Hetherington HP, Howe FA, Hüppi PS, Hurd RE, Kantarci K, Klomp DWJ, Kreis R, Kruiskamp MJ, Leach MO, Lin AP, Luijten PR, Marjańska M, Maudsley AA, Meyerhoff DJ, Mountford CE, Nelson SJ, Pamir MN, Pan JW, Peet AC, Poptani H, Posse S, Pouwels PJW, Ratai E-M, Ross BD, Scheenen TWJ, Schuster C, Smith ICP, Soher BJ, Tkáč I, Vigneron DB,

Kauppinen RA (2014) Clinical proton MR spectroscopy in central nervous system disorders. Radiology 270:658–679. https://doi.org/10.1148/radiol.13130531.

Riis-Vestergaard MJ, Laustsen C, Mariager CØ, Schulte RF, Pedersen SB, Richelsen B (2020) Glucose metabolism in brown adipose tissue determined by deuterium metabolic imaging in rats. Int J Obes 44:1417–1427. https://doi.org/10.1038/s41366-020-0533-7.

Rothman DL, Feyter HMD, de Graaf RA, Mason GF, Behar KL (2011) 13C MRS studies of neuroenergetics and neurotransmitter cycling in humans. NMR Biomed 24:943–957. https://doi.org/10.1002/nbm.1772.

Siesjö BK (1992) Pathophysiology and treatment of focal cerebral ischemia: Part I: Pathophysiology. J Neurosurg 77:169–184. https://doi.org/10.3171/jns.1992.77.2.0169.

Smith TAD (1998) FDG uptake, tumour characteristics and response to therapy: a review. Nucl Med Commun 19:97–106.

Sonnay S, Gruetter R, Duarte JMN (2017) How energy metabolism supports cerebral function: insights from 13C magnetic resonance studies in vivo. Front Neurosci 11. https://doi.org/10.3389/fnins.2017.00288.

Warburg O, Posener K, Negelein E (1924) The metabolism of cancer cells. Biochem Z 152:319–344.

(Received 17 November 2020, Accepted 13 January 2021)
(Available online xxxx)